Egyptian Journal of Chemistry

http://ejchem.journals.ekb.eg/

Electronic Structure, Global Reactivity Descriptors and Nonlinear Optical Properties of Some Novel pyrazolyl quinolinone Derivatives. DFT approach

EL-Shimaa Ibrahim[a], H. Moustafa*[b], Shimaa Abdel Halim[c]

[a] *Department of Chemistry, Faculty of Education, Ain Shams University, Roxy 11711, Cairo, Egypt*

[b] *Chemistry Department, College of Science, Cairo University, University Ave, Dokki, Giza, 12613, Egypt*

[c] *Department of Chemistry, Faculty of Education, Ain Shams University, Roxy 11711, Cairo, Egypt*

Abstract

The electronic and tautomeric structures of some novel pyrazolyl quinolinone derivatives are investigated using DFT/B3LYP/6-311++G (d, p) level of theory. The results of MO calculations show that all the studied compounds **1- 6** are planar, as indicated from the calculated dihedral angles. The calculated E_{HOMO} and E_{LUMO} energies of the studied compounds can be used to describe the extent of charge transfer in the studied molecules and to calculate the global properties; the chemical hardness (η), global softness (S), electrophilicity (ω), and electronegativity (χ). The effect of substituents of different strengths on the geometry, energetic and nonlinear optical properties are analyzed and discussed. The choice of these substituent's in the studied compounds aims at creating a push-pull system on pyrazolyl quinolinone structure which pave the way to understand their nonlinear optical properties. The calculated nonlinear optical parameters (NLO); polarizibilty (α), anisotropy of the polarizibility (Δα) and first order hyperpolarizibility (β) of the studied compounds have been calculated at the same level of theory and compared with the proto type Para-Nitro-Aniline (PNA), show promising optical properties. 3D- plots of the molecular electrostatic potential (MEP) for some of the studied compounds are investigated and analyzed showing the distribution of electronic charge density of orbitals . describing the electrophilic and nucleophilic sites of the selected molecules.

Keywords: B3LYP/6-311++G(d,p); DFT; NLO analysis; pyrazolyl quinolinone; global reactivity.

1.Introduction

quinolinone is an important structural item in several natural products and synthetic pharmaceuticals with wide range of biological activities including antibiotic, anticancer [1]anticancer drug applicant that strongly promotes cellapoptosis[2], antidepressant , anticonvulsant activities [3].,antipsychotic, antiallergic, antihistaminic or anti-inflammatory[4]–[6]. These broad biological activities have been a great concern in the field of pharmaceutical chemistry, thus numerous synthetic quinolinone anti-bacterial agents have been developed and various diseases have been treated with these drugs in clinical trials [7]**.**

Studying the electronic structure of these molecules aims to understand the forces that govern the electronic structure of the proposed molecules. In the literature there is no systematic study of the electronic structure and substituent effect, such a study is very important in understanding their electronic structure which may correlate with their activity.

The electronic structure of the novel compounds pyrazolyl quinolinone derivatives **1-6** and NLO analysis which have been evaluated to understanding of the electronic polarization underlying the molecular NLO processes [8,9]. Reliable structure-

*Corresponding author e-mail: husseinmam@hotmail.com.; (H. Moustafa).

Receive Date: 08 November 2021, Revise Date: 07 March 2022, Accept Date: 10 April 2022.

DOI: 10.21608/EJCHEM.2022.104957.4843

property relationships, where property here refers to linear polarizability (α), and first-(β) are required for the rational design of optimized materials for photonic devices such as electrooptic modulators and all-optical switches [10]. Our study in this work is to shed more light on the geometrical parameters (bond lengths, bond angles and dihedral angles), ground state properties of pyrazolyl quinolinone derivatives, energy gaps (highest occupied molecular orbital (HOMO), lowest unoccupied molecular orbital (LUMO), effect of substituent's of different electron donating- withdrawing power in the aryl moiety, and electrostatic potential are calculated using B3LYP/6-311++G (d,p). The electronic dipole moment (μ), and first order hyperpolarizibility (β) values of the studied compounds have been computed to study the NLO properties to identify and characterize the forces that govern the structure activity and the optical properties of the studied compounds. Finally, global reactivity descriptors including electronegativity (χ), hardness (η), softness (S), and electrophilicity (ω) of the studied compounds were calculated and analysed, while molecular electrostatic potential (MEP) of molecules were explored as well.

2. Experimental details

2.1. Synthesis

The titled compound and It's derivatives have been prepared as mentioned[11] were, compound **1** (E)-1-ethyl-4-hydroxy-3-(3-hydroxy-4-(phenyldiazenyl)-1H-pyrazol-5-yl)quinolin-2(1H)-one, compound **2** (E)-1-ethyl-4-hydroxy-3-(3-hydroxy-4-(p-tolyldiazenyl)-1H-pyrazol-5-yl)quinolin-2(1H)-one , compound **3** (E)-1-ethyl-4-hydroxy-3-(3-hydroxy-4-((4-methoxyphenyl)diazenyl)-1H-pyrazol-5-yl)quinolin-2(1H)-one, compound **4** (E)-3-(4-((4-chlorophenyl)diazenyl)-3-hydroxy-1H-pyrazol-5-yl)-1-ethyl-4-hydroxyquinolin-2(1H)-one ,compound **5** (E)-1-ethyl-4-hydroxy-3-(3-hydroxy-4-((4-nitrophenyl)diazenyl)-1H-pyrazol-5-yl)quinolin-2(1H)-one and compound **6** (E)-3-(4-((4-bromophenyl)diazenyl)-3-hydroxy-1H-pyrazol-5-yl)-1-ethyl-4-hydroxyquinolin-2(1H)-one as shown .

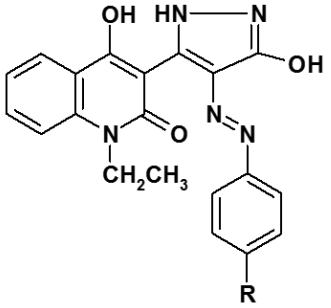

Compounds	R
1	**H**
2	**CH_3**
3	**OCH_3**
4	**Cl**
5	**NO_2**
6	**Br**

2.2. Computational details

All computations were carried out using Khon-Sham's DFT method subjected to the gradient-corrected hybrid density functional B3LYP method [11, 12]This function is a combination of the Becke's three parameters non-local exchange potential with the non-local correlation functional of Lee et al[13, 14].For each structure, a full geometry optimization was performed using this function[11,12]and the 6-311++G (d, p) basis set[16] as implemented by Gaussian 09 package[17]. All geometries were [١٨]visualized either using GaussView 5.0.9 or chemcraft 1.6[19] software packages. No symmetry constrains were applied during the geometry optimization. Also, the total static dipole moment (μ), $\langle\Delta\alpha\rangle$, and $\langle\beta\rangle$, values were calculated by using the following equations [19, 20].

$\mu = (\mu 2x + \mu 2y + \mu 2z)\ 1/2,$

$,\langle\alpha\rangle = 1/3\ (\alpha xx + \alpha yy + \alpha zz)$

$\Delta\alpha = ((\alpha x\mathrm{x} - \alpha yy)\ 2 + (\alpha yy - \alpha zz)\ 2 + (\alpha zz - \alpha xx)\ 2/2)1/2$

$$\langle\beta\rangle = (\beta 2 + \beta 2y + \beta 2z)\ 1/2 \quad (1)$$

Where

$$\beta x = \beta xxx + \beta xyy + \beta xzz,$$
$$\beta y = \beta yyy + \beta xxy + \beta yzz,$$
$$\beta z = \beta zzz + \beta x\ z + \beta yyz. \quad (2)$$

HOMO and LUMO energy values, electronegativity, and chemical hardness can be calaulated as follows : $\chi = (I+A)/2$ (electronegativity), $\eta = (I-A)/2$

(chemical hardness), $S = 1/2\eta$ (globalsoftness),$\omega = \mu 2/2\eta$ (electrophilicity) where I and A are ionization potential and electron affinity, and $I = -E$HOMO and $A = -E$LUMO, respectively [22][10].For the conversion factors of α, β, and HOMO and LUMO energies in atomic and CGS units: 1 atomic unit (a.u.) = 0.1482 $\times 10^{-24}$ electrostatic unit (esu) for polarizability $\langle\alpha\rangle$; 1 a.u. = 8.6393×10^{-33} esu for first hyperpolarizability $\langle\beta\rangle$; 1 a.u. = 27.2116 eV for HOMO and LUMO energies.

3.Results and Discussion

3.1. Electronic structure

3.1.1. tautomeric structure

The novel prepared pyrazolyl quinolinone exists in two π-isoelectronic structures **I** and **II**. DFT calculations at B3LYP/6-311++G** level of theory were used to investigate which form is more stable at the ground state. The optimized geometry of the studied tautomeric structure was checked as minima on the potential energy surface by frequency calculations using the same level of calculation. Structure optimization for the studied tautomeric structure is presented in Fig. 1. The optimization of the tautomeric structure show that the molecules belong to C1 symmetry point group. Total energy, energy of HOMO and LUMO, energy gap and dipole moment of the two tautomeric structures computed at the B3LYP/6-311++G(d,P) are presented in Table 1. The results of MO- computation predicted that the total energy of **I** is -1272.13547 au and that for **II** is -1272.13578 au. On the energy scale, the tautomeric structures exist in a static mixture in the ground state with structure **II** (OH) is more stable than structure **I** (C=O) by 0.813 kJ (c.f. Table1). The energy gap of **II** is less than **I** by 0.05 $kJmol^{-1}$, indicating that tautomer **II** is chemically active than tautomer **I**. Also, the dipole moment which measures the polarization of the molecule, indicating that tautomer **II** is more polarized than tautomer **I** by 4.1D. Therefore, structure **II** in the statically mixtures in the ground state is considered the major product and all calculations in this paper considered the enol-structure is the stable form in the ground state.

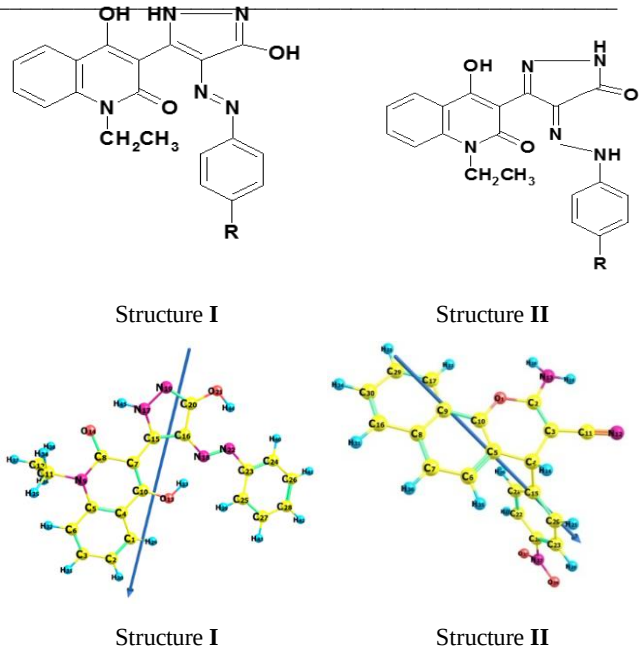

Fig. 1. The optimized geometry of the two tautomeric structures

Table 1
Total energy, energy of HOMO and LUMO, energy gap and dipole moment of the two tautomer structures computed at the B3LYP/6-311++G(d,P) .

Compounds	Structure **I**	Structure **II**
E_T (au)	-1272.13547	-1272.13578
E_{HOMO} (eV)	-6.0501	-6.1654
E_{LUMO} (eV)	-2.7521	-2.8680
E_{gap} (eV)	3.298	3.2974
μ (Debye)	2.8087	6.8841

3.1.2. Geometry structure

The optimized structures and the vector of the dipole moment of the studied compounds **1-6** using the B3LYP/6- 311++G (d, p) are presented in Fig 2. The energies of HOMO, LUMO, energy gap and dipole moment of all compounds are presented in Fig. 3and Table 2. The optimized geometrical parameters (bond lengths, bond angles and dihedral angles) of the studied compounds **1-6**, are listed in Table3 with the available experimental data. The analysis of Table 3 and Fig. 2 shows that the most stable geometry of the studied compounds, **1-6**, is the planar structures as indicating from the dihedral angles c.f. Table 3. The calculated bond lengths and bond angles for the studied compounds, **1-6** using B3LYP/6-311++ G (d,p) are in good agreement with the reported x-ray data [23].

Table 2

Total energy, energy of HOMO and LUMO, energy gap, dipole moment, the ionization potential (I ,eV), electron affinity (A ,eV), chemical hardness (η , eV), global softness (S,eV^{-1}), chemical potential (V,eV^{-1}), electronegativity (χ,eV), and global electrophilicity index, (ω,eV), of the studied compounds **1-6** computed at the B3LYP/6-311++G (d,P) level of theory.

Parameters	Compound **1**	Compound **2**	Compound **3**	Compound **4**	Compound **5**	Compound **6**
E_T(a.u)	-1272.13578	-1311.4640	-1386.6919	-1731.7581	-1476.6972	-3845.6777
E_{HOMO} (a.u)	-6.1654	-6.0689	-6.0991	-6.2416	-6.4159	-6.2429
E_{LUMO} (a.u)	-2.8680	-2.7930	-2.8157	-3.0157	-3.2371	-3.026
Energy gap = $\|E_{HOMO} - E_{LUMO}\|$ eV	3.2974	3.2760	3.2833	3.2259	3.1789	3.2169
μ(debye)	6.8841	7.1934	7.6322	6.4284	3.0738	6.4416
Ionization potential (I=-E_{HOMO})eV	6.1654	6.0689	6.0991	6.2416	6.4159	6.2429
Electron affinity (A=-E_{LUMO}) eV	2.8680	2.7930	2.8157	3.0157	3.2371	3.026
Electronegativity χ=(I+A)/2 eV	4.5167	4.4309	4.4574	4.7338	4.8265	4.6345
chemical potential p= - χ eV	-4.5167	-4.4309	-4.4574	-4.7338	-4.8265	-4.6345
Chemical Hardness (η=(I-A)/2) eV	1.6487	1.6380	1.6417	1.6130	1.5894	1.6085
Chemical softness (S=1/2η) eV	0.3033	0.3053	0.3046	0.3099	0.3146	0.3109
Electrophilicity index ω= $\mu^2/2\eta$ eV	6.1868	5.9931	6.0513	6.9464	7.3281	34.1608

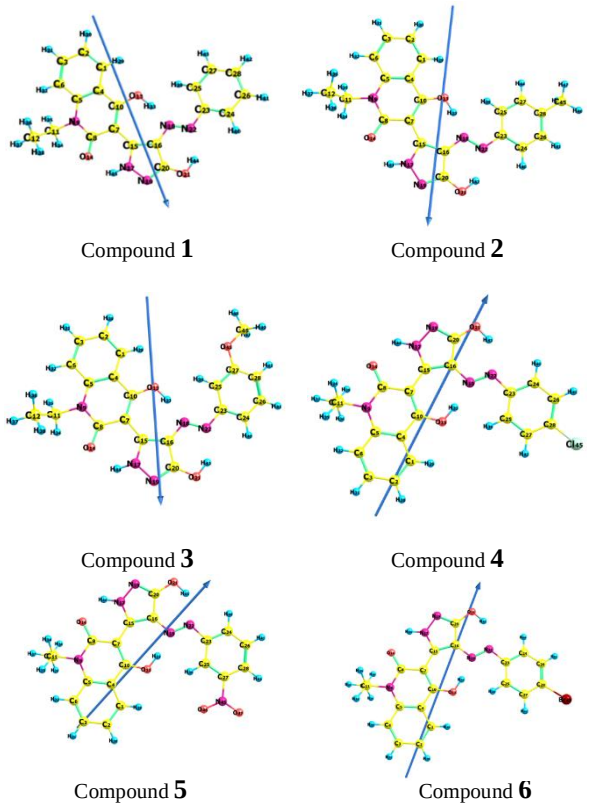

Compound **1** Compound **2**

Compound **3** Compound **4**

Compound **5** Compound **6**

Fig. 2. The optimized structure, perspective view of dipole moment of the studied compounds **1-6** at B3LYP/6-311++ G (d, p).

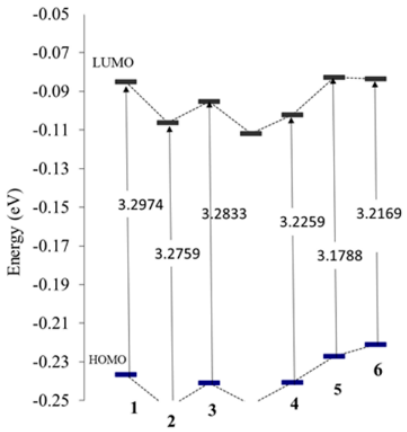

Fig.3. Energy of HOMO, LUMO and energy gap of the studied compounds **1-6** at B3LYP/6-311++ G (d, p) level of theory.

Table 3
Optimized geometrical parameters bond lengths (Å), bond angles (degrees)and dihedral angles(degrees) of compounds**1-6**calculated at B3LYP/6-311++ G(d,p) level.

	Compound **1**	Compound **2**	Compound **3**	Compound **4**	Compound **5**	Compound **6**	Experimental [a]
Bond lengths(Å)							
C26-H41	1.084	1.085	1.084	1.082	1.083	1.082	1.000
C24-C26	1.390	1.389	1.386	1.389	1.390	1.389	1.396
C24-C23	1.403	1.402	1.405	1.403	1.404	1.402	1.40
C23-C25	1.405	1.406	1.398	1.406	1.403	1.406	1.40
C23-N22	1.408	1.406	1.408	1.405	1.407	1.405	1.41
N22-N18	1.275	1.275	1.275	1.276	1.278	1.276	1.33
N18-C16	1.358	1.360	1.358	1.357	1.351	1.357	1.35
C16-C20	1.437	1.436	1.437	1.438	1.441	1.438	1.40
C20-O21	1.334	1.334	1.334	1.334	1.333	1.333	1.359
O21-H44	0.982	0.982	0.982	0.981	0.981	0.981	0.92
C20-N19	1.311	1.312	1.311	1.311	1.309	1.311	
N19-N17	1.364	1.364	1.365	1.365	1.367	1.365	1.394
N17-H45	1.016	1.016	1.016	1.016	1.017	1.016	
N17-C15	1.347	1.348	1.347	1.347	1.345	1.347	1.34
C15-C7	1.464	1.465	1.464	1.464	1.462	1.464	1.520
C7-C10	1.392	1.391	1.392	1.392	1.393	1.392	1.386
Bond angles(^{0})							
C24-C26-C28	120.0	121.1	121	119	120.4	119.1	121.0
C26-C28-C27	119.7	117.9	119.2	121	118	121	119.8
C28-C27-C25	120.7	121.8	120.4	119.7	123	119.7	120.3
C27-C25-C23	119.7	119.9	119.8	120.2	118.4	120.2	119.40
C25-C23-C24	119.4	118.7	119.9	119	119.2	119.0	119.40
C25-C23-N22	125.2	125.7	125	125.6	125.3	125.5	125.3
C23-N22-N18	117.3	117.6	117.6	117.4	117	117.3	
N22-N18-C16	116.8	116.8	116.7	116.8	117	116.8	
N18-C16-C20	127.4	127.4	127.3	127.4	127.4	127.4	
C16-C20-O21	125.5	125.5	125.5	125.5	125.5	125.5	122.10
C16-C20-N19	111.6	111.7	111.6	111.6	111.6	111.6	
N19-C20-O21	28.9	28.8	28.8	28.9	28.8	122.8	
C20-N19-N17	104.3	104.3	104.3	104.3	104.3	104.3	
N19-N17-C15	115.8	115.7	115.8	115.8	115.9	115.8	
N19-N17-H45	122	122	122	122	122	122	
O14-C8-N9	118.3	118.3	118.3	118.3	118.5	118.3	
C8-N9-C11	116.1	116.2	116.1	116.1	116.1	116.1	116.2
C8-N9-C5	122.9	122.9	122.9	122.9	122.9	122.8	122.49
Dihedral angles(^{0})							
C23-C25-C27-C28	0	0.1	0.1	-0	0	0	
H39-C25-C23-C24	178.4	-179.6	-179.2	-180	179.4	179	
N22-N18-C16-C15	179.2	179.9	-179.3	-180	179.7	179.5	
O21-C20-C16-C15	180	-180	-180	-180	-180	-180	179.20
C24-C23-N22-N18	170.4	-180	-174.8	-179.7	176.1	174.1	
H45-N17-N19-C20	179.4	-179.7	180	-179.9	-179.9	179.6	
C 16-C15-C7-C8	178.3	-180	179.5	179.6	179.5	178.7	
O14-C8-N9-C5	176.3	177	176.9	177	177.1	176.5	
H33-O13-C10-C4	-179.3	179.5	-179.7	180	-180	-179.4	
C8-N9-C5-C6	-176.2	-176.8	-176.8	-177	-177.1	-176.5	
C5-N9-C11-C12	-86.5	-86.1	-86.2	-86.1	-85.9	-86.1	
C10-C4-C1-C2	-179.5	-179.4	-179.5	-179.5	-179.5	-179.6	175.3

[a]X-ray data of compounds**1-6** from Ref.[24]

3.1.3. Ground state properties

Total energy, energy of HOMO and LUMO, energy gap, dipole moment, the ionization potential (I ,eV), electron affinity (A ,eV), chemical hardness (η , eV), global softness (S,eV^{-1}), chemical potential (V,eV^{-1}), electronegativity (χ,eV), and global electrophilicity index, (ω,eV), of the studied compounds **1-6** computed at the B3LYP/6-311++G (d,P) level of theory are listed in Table 2. The ionization energy, I.E, of compound **1** which measures the donating property (oxidation power) is 6.17eV c.f. Table 2. The effect of substituents of different strengths and hence in the donating properties follows the order: **2** > **3** > **1** > **4** > **6** > **5** as shown in Table 2. However, the electron affinity, E.A., of **1** which measures the accepting property (reducing power) is 2.87 eV. The order of accepting properties of pyrazolyl quinolinone derivatives compounds follows **2** < **3** < **1** < **4** < **6** < **5** as shown in Table2. The band gap, Egap, is the energy difference between EHOMO and ELUMO, it signifies the facile electron transition from HOMO to LUMO and characterizes the molecular chemical stability which is an urgent parameter for studying the molecular electrical transition. From the results in Table 2 and Fig. 3 shows that the computed reactivity in the gas phase of the studied compounds increases in the order: **5** > **6** > **4** > **2** > **3** > **1**. This indicates that the smaller the Egap, the high er the reactivity of these compounds. Finally, the theoretically computed dipole moment, μ, for compound **1** which measures the charge separation over the molecule is 6.88D. The general trend of the dipole moment changes for the studied pyrazolyl quinolinone derivatives follow the order **3** > **2**> **1**> **6** > **4** > **5** c.f. Table2 and the vector of the dipole moment is presented in Fig. 2.

3.1.4. Global reactivity descriptors

They include chemical hardness(η), electronegativity (χ), chemical potential (V), electrophilicity (ω), electron affinity (A), ionization potential(I) and global softness (S) which are calculated at B3LYP/6- 311++G (d,p) c.f. Table 2. The frontier molecular orbital (FMO) energies were calculated for the studied compounds at the same level of theory. Using HOMO and LUMO energies, ionization potential and electron affinity can be expressed as I~ -EHOMO, A~ -ELUMO at the B3LYP/6-311++G (d,p) as shown in Table 2. The variation of electronegativity (χ) values is supported by electrostatic potential, for any two molecules, where electron will be partially transferred from one of low χ to that of high χ. The results show that the order of decreasing χ is: **5** > **4** > **6**> **1** > **3** > **2**. The results of small η values for the studied compounds reflect the ability of charge transfer inside the molecule. Therefore, the order of charge transfer inside the molecule is: **1**> **3** > **2**> **4** > **6** > **5**. There is a linear relationship between η and Eg as shown in Table 2. Considering η values, the higher the η values, the harder is the molecule and vice versa.

3.1.5. Natural Charge

The natural population analysis [25] done on the electronic structures of compounds **1-6** clearly describes the distribution of electrons in various sub-shells of their atomic orbits. The accumulation of charges on the individual atom presented in Table 4. In case of our studied compounds **1-6**, the most negative centres are O13, O14, O21, N9, N17, N18, N19, N22 atoms. According to an electrostatic point of view of the molecule, these negative atoms have tendency to donate an electron. Whereas, the most electropositive atoms such as; C8, C10 have tendency to accept an electron.

3.2. *Nonlinear optical (NLO) Analysis*

In the literature no experimental or theoretical investigations were found titled NLO for these classes of molecules. NLO is at the forefront of current research due to its importance in providing key functions of frequency shifting, optical modulation, switching, laser, fibre, optical materials logic and optical memory for the emerging technologies in areas such telecommunications, signal processing and optical inter connections [26]–[28]. In order to investigate the relationship between molecular structure and NLO, the polarizabilities and hyperpolarizabilities of the studied compounds **1-6** are calculated using DFT/B3LYP/6-311++G(d,p). Total static dipole moment (μ), the mean polarizability α, the anisotropy of the polarizability Δα, the mean first-order hyperpolarizability (β) of the studied compounds

1-6 are listed in Table 5. P-nitro aniline (PNA) is a standard prototype molecule used in NLO studies. In this study, PNA is chosen as a reference as there were no experimental values of NLO properties of the studied compounds. The values of β in Table 5 show that the order of increasing with respect to PNA is : compound **1**is ~79 times higher than (PNA),whereas compound **2** is ~ 85 times higher than (PNA), compound **3** is ~ 130.5 times higher than the standard (PNA) , compound **4** is ~ 188.5 times higher than the standard (PNA) ,compound **5** is ~ 80 times higher than the standard (PNA) and compound **6** is ~ 126 times higher than the standard (PNA). The calculated first order hyperpolarizability of p- nitroaniline (PNA) is 15.5×10^{-30} esu [29]–[31]. The analysis of the β parameter show that the studied compounds show promising optical properties.

Table 4
Natural Charge for the studied compounds **1-6** computed at the B3LYP/6-311++G(d,P) level of theory.

Compounds	**1**	**2**	**3**	**4**	**5**	**6**
			Natural charge			
C5	0.2209	0.2072	0.2047	0.2052	0.2250	0.2234
N9	-0.4541	-0.4613	-0.4586	-0.4592	-0.4483	-0.4512
C8	0.6761	0.6348	0.6407	0.6298	0.6761	0.6757
O14	-0.6875	-0.7010	-0.6969	-0.7014	-0.6876	-0.6869
C10	0.4419	1.2303	1.2484	1.2392	0.5799	0.5742
O13	-0.6929	-0.7866	-0.7628	-0.7712	-0.7083	-0.7165
C15	0.1907	0.0889	0.1140	0.0446	0.2028	0.1941
N17	-0.3079	-0.3149	-0.3272	-0.4694	-0.3292	-0.3301
N19	-0.3238	-0.3255	-0.3215	-1.1238	-0.2866	-0.2883
C20	0.4917	0.4890	0.4924	0.1545	0.4841	0.4816
O21	-0.6584	-0.6601	-0.6590	-0.6957	-0.6557	-0.6583
N18	-0.2371	-0.2491	-0.2511	-0.2604	-0.2310	-0.2382
N22	-0.2874	-0.2838	-0.2720	-0.2958	-0.3070	-0.2930
C23	0.1091	0.1013	0.1196	0.1044	0.1204	.01049
C45		-0.5914				
O45			-0.5393			
C46			-0.2051			
Cl45				0.0134		
N45					0.4864	
O46					-0.3749	
O47					-0.3742	
Br45						0.0779

Table 5

Total static dipol moment (μ), the mean polarizability (<α>), the anisotropy of the polarizability (Δα), and the mean first-order (<**β**>), of the studied compounds **1-6** computed at B3LYP/6-311++ G (d,P).

Property	**PNA**	**1**	**2**	**3**	**4**	**5**	**6**
μ_x, D		-2.3494	0.0570	0.3732	4.6134	2.1690	2.4436
μ_y, D		6.0590	-6.4489	7.5473	-4.4141	-2.7869	-5.9601
μ_z, D		0.6925	0.1430	0.0405	0.6287	1.7008	-0.0016
μ, Debye [a]	2.44	6.54	6.45	7.56	6.42	3.92	6.44
α_{XX}, a.u.		-126.5956	-141.0215	-126.6804	-166.3305	-143.0077	-157.0337
α_{XY}, a.u.		3.8613	5.2511	1.4709	-26.3572	-27.3843	-22.7624
α_{YY}, a.u.		-174.6451	-181.4819	-187.0076	-193.2902	-207.5318	-195.5132
α_{ZZ}, a.u.		-167.2590	-174.1348	-15.2258	-179.5923	-183.0430	-185.4813
α_{YZ}, a.u.		-3.3301	-4.5380	-1.6823	1.6936	-2.1794	1.3738
α_{XZ}, a.u.		4.5058	7.6767	0.0243	-5.2194	-8.8924	-1.0583
$<\alpha>\times10^{-24}$esu [b]	22	-23.1439	-24.5339	-24.3728	-26.6372	-26.3590	-26.5786
$\Delta\alpha\times10^{-24}$esu		6.86746	6.13744	8.4696	7.7286	11.1733	7.784
βxxx,a.u.		-13.6876	-3.9527	84.9972	295.1138	29.8012	-0.4216
βxxy,a.u.		55.0362	109.8700	109.8700	72.5099	46.4051	-46.5447
βxyy,a.u.		-24.2034	-23.3218	32.9574	39.7769	67.7682	-77.2802
βyyy,a.u.		140.6252	-152.9144	218.2885	-165.6272	-140.5019	-225.3207
βxxz,a.u.		19.9018	10.4943	-3.0764	25.3768	45.2000	1.9594
βxyz,a.u.		-12.0081	-35.3579	-1.7416	-4.1035	14.4701	-2.6540
βyyz,a.u.		6.0570	3.8315	3.2894	7.3343	27.7752	3.1033
βxzz,a.u.		-7.0274	4.2605	-3.7875	2.5330	-2.7043	-61.9004
βyzz,a.u.		-24.4419	16.6667	-12.7549	17.2442	13.9051	2.1778
βzzz,a.u.		-0.8224	0.5405	-2.5923	-5.7365	-10.7187	0.8682
$<\beta>\times10^{-30}$esu [c]	15.5	1220.67	1321.52	2023.90	2924.09	1244.29	1946.63

3.3. Molecular electrostatic potential

The electronic density is correlated by Molecular electrostatic potential (MEP) and is a very good descriptor in understanding sites for electrophilic and nucleophilic attack as well as hydrogen bonding interactions [32]. This is correlated with dipole moments, electro-negativity, partial charges, and chemical reactivity of the molecules. These maps allow us to visualize variably charged regions of a molecule by the knowledge of the charge distributions can be used to determine how molecules interact with one another. The calculated 3D MEP and ESP of some of the studied molecules **1,3,4** and **5** are calculated from optimized molecular structure using DFT/B3LYP/6- 311++G (d,p) as shown in Fig. 4 . The results show that , in case of 1 (X=H) the negative region (red) is mainly over the O atomic sites, which is caused by the contribution of lone-pair electron of oxygen atom while the positive (blue) potential sites are around the hydrogen, and carbon atoms. A portion of the molecule that has negative electrostatic potential will be susceptible to electrophilic attack—the more negative the higher the

tendency for electrophilic attack. The colour scheme for the MEP surface is as follows: red for electron rich, (partially negative charge); blue for electron deficient, (partially positive charge); light blue for (slightly electron deficient region); yellow for (slightly electron rich region); green for neutral (zero potential) respectively. Potential increases in the following order: red < orange < yellow < green < blue [33] [34].

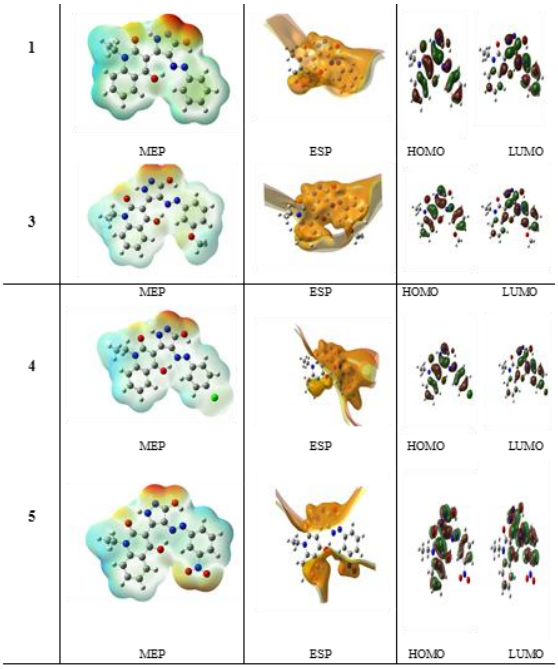

Fig.4. Molecular surfaces of some studied compounds **1,3,4** and **5** at B3LYP/6-311++G (d, p).

4. Conclusion

The electronic and tautomeric structures of some novel pyrazolyl quinolinone derivatives are investigated using DFT/B3LYP/6-311++G (d, p) level of theory. Structure **II (OH)** in the statically mixtures in the ground state is considered the major product and all calculations in this paper considered the enol-structure is the stable form in the ground state. The order of the donating property (oxidation power) of the studied compounds is **2** > **3** > **1** > **4** > **6** > **5,** whereas that of the accepting property (reducing power) is **2** < **3** < **1** < **4** < **6** < **5.** Also, the results of the MO calculation shows that the computed reactivity in the gas phase of the studied compounds increases in the order: **5** > **6** > **4** > **2** > **3** > **1.** The results of the calculated global properties show that the order of decreasing χ(electronegativity) is: **5** > **4** > **6**> **1** > **3** > **2**. The small η values for the studied compounds reflect the ability of charge transfer inside the molecule. Therefore, the order of charge transfer inside the molecule is: **1**> **3** > **2**> **4** > **6** > **5**. There is a linear relationship between η and Eg for the studied compounds. In case of our studied compounds **1-6**, the most negative centres are O13, O14, O21, N9, N17, N18, N19, N22 atoms, these negative atoms have tendency to donate an electron. Whereas, the most electropositive atoms such as; C8, C10 have tendency to accept an electron. The mean first-order hyperpolarizability (β) of the studied compounds **1-6** calculated at the same level of calculation and compared with P-nitro aniline (PNA) as a reference molecule show that compound **1**is ~79 times higher than (PNA),whereas compound **2** is ~ 85 times higher than (PNA), compound **3** is ~ 130.5 times higher than the standard (PNA) , compound **4** is ~ 188.5 times higher than the standard (PNA) ,compound **5** is ~ 80 times higher than the standard (PNA) and compound **6** is ~ 126 times higher than the standard (PNA). The analysis of the β parameter show that the studied compounds show promising optical properties.

5. References

[1] A. K. Kabi *et al.*, "HFIP-mediated strategy towards β-oxo amides and subsequent Friedel-Craft type cyclization to 2-quinolinones using recyclable catalyst," *Tetrahedron Lett.*, vol. 61, no. 46, p. 152535, 2020, doi: 10.1016/j.tetlet.2020.152535.

[2] V. P. Hradil, P. Krejci, J. Hlavac, I. Wiedermannova, A. Lycka, "Synthesis Bertolasi, NMR spectra and X-ray data of chloro and dichloro derivatives of 3-hydroxy-2-phenylquinolin-4(1H)-ones and their cytostatic activity," *Heterocycl. Chem.*, vol. 41, pp. 375–379, 2004.

[3] X. Q. Deng, M. X. Song, Y. Zheng, and Z. S. Quan, "Design, synthesis and evaluation of the antidepressant and anticonvulsant activities of triazole-containing quinolinones," *Eur. J. Med. Chem.*, vol. 73, pp. 217–224, 2014, doi: 10.1016/j.ejmech.2013.12.014.

[4] R. S. S. Carradori, "New frontiers in selective human MAO-B inhibitors," *Med. Chem*, vol. 58, pp. 6717–6732, 2015.

[5] L. Pescatori *et al.*, "N-Substituted Quinolinonyl

Diketo Acid Derivatives as HIV Integrase Strand Transfer Inhibitors and Their Activity against RNase H Function of Reverse Transcriptase," *J. Med. Chem.*, vol. 58, no. 11, pp. 4610–4623, 2015, doi: 10.1021/acs.jmedchem.5b00159.

[6] S. Hadida *et al.*, "Discovery of N -(2,4-Di- tert - butyl-5-hydroxyphenyl)-4-oxo-1,4-dihydroquinoline-3-carboxamide (VX-770, Ivacaftor), a potent and orally bioavailable CFTR potentiator," *J. Med. Chem.*, vol. 57, no. 23, pp. 9776–9795, 2014, doi: 10.1021/jm5012808.

[7] P. S. A.M. Birch, P.W. Kenny, N.G. Oikonomakos, L. Otterbein and D. P. W. P.R.O. Whittamore, "Development of potent, orally active 1- substituted-3,4-dihydro-2-quinolone glycogen phosphorylase inhibitors, Bioorg," *Med. Chem*, vol. 17, pp. 394–399, 2007.

[8] P. N. Prasad and D. J. Williams, "Nonlinear Optical Effects in Molecules and polymers," *John Wiley Sons, New York, NY, USA*, 1991.

[9] F. Meyers, S. R. Marder, B. M. Pierce, and J. L. Brédas, "Electric Field Modulated Nonlinear Optical Properties of Donor-Acceptor Polyenes: Sum-Over-States Investigation of the Relationship between Molecular Polarizabilities (α,β, and γ.) and Bond Length Alternation," *J. Am. Chem. Soc.*, vol. 116, no. 23, pp. 10703–10714, 1994, doi: 10.1021/ja00102a040.

[10] N. Günay, H. Pir, D. Avci, and Y. Atalay, "NLO and NBO analysis of sarcosine-maleic acid by using HF and B3LYP calculations," *J. Chem.*, pp. 1–16, 2013, doi: 10.1155/2013/712130.

[11] M. Abass, "CHEMISTRY OF SUBSTITUTED QUINOLINONES. PART I1 SYNTHESIS OF NOVEL 4-PYRAZOLYLQUINOLINONE DERIVATIVES," *Synth. Commun.*, vol. 30, no. 15, pp. 2735–2757, 2000, doi: 10.1080/00397919308020392.

[12] A. D. Becke, "Density-functional thermochemistry . III . The role of exact exchange," *Chem. Phys*, vol. 98, p. 5648, 1993, doi: 10.1063/1.464913.

[13] A. D. Becke, "A new mixing of Hartree–Fock and local density-functional theories," vol. 98, p. 1372, 1993, doi: 10.1063/1.464304.

[14] R. G. P. Lee, Choonkyu, W. Yang, "S-matrix generating functional and efFective action," vol. 37, no. 6, pp. 1485–1491, 1988.

[15] P. B. Miehlich, A. Savin, H. Stolt, H, "Results obtained with the correlation energy density functionals of becke and Lee, Yang and Parr," *Chem.Phys. Lett*, vol. 157, no. 3, pp. 200–206, 1989.

[16] "B. Stefanov, B. G. Liu, A. Liashenko, P. Piskorz, I. Komaromi R. L. Martin, D. J. Fox, T. Keith, M. A. Al-Laham, C. Y. Peng, A. Nanayakkara, M. Challacombe, P. M. W. Gill, B. Johnson, W. Chen M. W. Wong, C. Gonzalez, J. A. Pople, Gaussian, Inc., Pittsburg," 2003.

[17] "M. Frisch, J. G. W. Trucks, H. B. Schlegel, G, E. Scuseria, et al., Gaussian, Inc., Wallingford CT," 2009.

[18] "GaussView, Version 5, Dennington, R.; Keith, T.; Millam, J. Semichem Inc., Shawnee Mission KS," 2009.

[19] "http://www.chemcraftprog.com."

[20] D. Avcı, "Second and third-order nonlinear optical properties and molecular parameters of azo chromophores: Semiempirical analysis," *Spectrochim. Acta A*, vol. 82, pp. 37–43, 2011, doi: 10.1016/j.saa.2011.06.037.

[21] Y. A. D. Avci, A. Başoğlu, "Ab initio HF and DFT calculations on an organic non-linear optical material," *Struct. Chem.*, vol. 21, pp. 213–219, 2010, doi: 10.1007/s11224-009-9566-1.

[22] R. G. Pearson, "Absolute electronegativity and hardness correlated with molecular orbital theory," *Nati. Acad. Sci*, vol. 83, pp. 8440–8441, 1986.

[23] T. A. Farghaly, N. A. Abdel Hafez, E. A. Ragab, H. M. Awad, and M. M. Abdalla, "Synthesis, anti-HCV, antioxidant, and peroxynitrite inhibitory activity of fused benzosuberone derivatives," *Eur. J. Med. Chem.*, vol. 45, no. 2, pp. 492–500, 2010, doi: 10.1016/j.ejmech.2009.10.033.

[24] H. . M. E. H. Moustafa, HusAbdelrahim. Z. Moussab, Mohamed E. Elshakrea, "DFT, Electronic absorption spectra and Non-linear optical properties of some 4H-benzo[h]chromene Derivatives. Solvent effect and TD-DFT Approach," *Egypt. J. Chem.*, vol. 0, no. 0, pp. 0–0, 2021, doi: 10.21608/ejchem.2021.69996.3544.

[25] A. E. Reed, R. B. Weinstock, and F. Weinhold, "Natural population analysis," *J. Chem. Phys.*, vol. 83, no. 2, pp. 735–746, 1985, doi: 10.1063/1.449486.

[26] S. Natarajan, G. P. Chitra, S. A. Martin Britto Dhas, and S. Athimoolam, "Growth, structural, thermal and optical studies on L-glutamic acid hydrobromide - A new semiorganic NLO material," *Cryst. Res. Technol.*, vol. 43, no. 7, pp. 713–719, 2008, doi: 10.1002/crat.200711089.

[27] M. P. Lytle, R. S., Hom, P. W., & Mokwa, "Information To Users Umi," *Dissertation*, vol. Ph.D. Thes, no. Structural Biology and Molecular Biophysics, University of Pennsylvania, PA, USA., p. 274, 1998.

[28] D. S. Bradshaw and D. L. Andrews, "QUANTUM CHANNELS IN NONLINEAR OPTICAL PROCESSES DAVID," *Nonlinear Opt. Phys. Mater.*, vol. 18, no. 2, pp. 285–299, 2009.

[29] L. T. Cheng, W. Tam, S. H. Stevenson, G. R. Meredith, G. Rikken, and S. R. Marder, "Experimental investigations of organic molecular nonlinear optical polarizabilities. 1. Methods and results on benzene and stilbene derivatives," *J. Phys. Chem.*, vol. 95, no. 26, pp. 10631–10643, 1991, doi: 10.1021/j100179a026.

[30] F. L. Huyskens, P. L. Huyskens, and A. P. Persoons, "Solvent dependence of the first hyperpolarizability of p-nitroanilines: Differences between nonspecific dipole-dipole interactions and solute-solvent H-bonds," *J. Chem. Phys.*, vol. 108, no. 19, pp. 8161–8171, 1998, doi: 10.1063/1.476171.

[31] T. Gnanasambandan, S. Gunasekaran, and S. Seshadri, "Experimental and theoretical study of p-nitroacetanilide," *Spectrochim. Acta - Part A Mol. Biomol. Spectrosc.*, vol. 117, pp. 557–567, 2014, doi: 10.1016/j.saa.2013.08.061.

[32] E. Scrocco and J. Tomasi, *Electronic Molecular Structure, Reactivity and Intermolecular Forces: An Euristic Interpretation by Means of Electrostatic Molecular Potentials*, vol. 11, no. C. 1978.

[33] P. Politzer and J. S. Murray, "The fundamental nature and role of the electrostatic potential in atoms and molecules," *Theor. Chem. Acc.*, vol. 108, no. 3, pp. 134–142, 2002, doi: 10.1007/s00214-002-0363-9.

[34] D. Sajan, L. Joseph, N. Vijayan, and M. Karabacak, "Natural bond orbital analysis, electronic structure, non-linear properties and vibrational spectral analysis of l-histidinium bromide monohydrate: A density functional theory," *Spectrochim. Acta - Part A Mol. Biomol. Spectrosc.*, vol. 81, no. 1, pp. 85–98, 2011, doi: 10.1016/j.saa.2011.05.052.